

CHARACTERISTICS OF MICROBURST EVENTS OBSERVED WITH THE NATIONAL WEATHER RADAR TESTBED PHASED ARRAY RADAR

Travis M. Smith, Pamela L. Heinselman, and David Priegnitz

Cooperate Institute for Mesoscale Meteorological Studies, University of Oklahoma
(also affiliated with NOAA / National Severe Storms Laboratory)

1. Introduction

Heinselman et al. (2006) examine the evolution of several storm events utilizing high-temporal-resolution phased array radar data. This study extends their work, with a focus on rapidly evolving convective wind events. Microbursts are small-scale (< 4 km diameter) outflows induced by strong downdrafts in thunderstorms that frequently cause damage to property and are a hazard to aviators. Many severe microbursts originate from storm cells that form in regions of moderate-to-high Convective Available Potential Energy (CAPE), weak environmental shear, and environments that are highly unstable to downdraft formation. These storm cells typically have a life cycle of 20–40 minutes, which makes them very difficult to predict.

Automated algorithms that analyze radar data and make short-term predictions for microburst events, as well as detecting low-altitude divergence signatures associated with their outflows, have been created for WSR-88D and TDWR systems (Smith et al. 2004; Wolfson et al. 1994). These applications rely on microburst “precursors” that may be observed at higher altitudes of a storm shortly preceding the outflow at the surface to make short-lead-time forecasts of a microburst event. Some precursors identified in prior studies (Roberts and Wilson 1989; Eilts et al. 1996) include rapidly descending reflectivity cores that frequently start at an altitude higher than other storms in the same environment, and strong, deep convergence at mid-altitudes of the storm. However, microburst events evolve rapidly, and because these radars typically only sample the upper portions of a storm once every 4 to 6 minutes (depending on scanning strategy), they may or may not sample key precursor features aloft or the outflow produced near the surface.

This manuscript examines damage-producing severe microburst events that occurred in Central Oklahoma on 10 and 11 July 2006 that were observed with the National Weather Radar Testbed (NWRT) Phased Array Radar (PAR). These storms formed within 60 km of the PAR site and were sampled with a temporal resolution of approximately 30 seconds. We compare the PAR observations of the storms with data collected by Oklahoma City WSR-88D (KTLX) and Oklahoma City Terminal Doppler Weather Radar (OKC TDWR).

2. Data sources

Data were collected with the KTLX WSR-88D, the OKC TDWR, and the NWRT PAR. The WSR-88D operated in Volume Coverage Pattern (VCP) 12 on both days, while the NWRT utilized the same elevation angles but at a scanning rate approximately 7.5 times faster than KTLX. The TDWR operated with an interlaced VCP, scanning at the lowest elevation angle once per minute and the entire volume once every 3.5 minutes. Table 1 compares the radar sampling characteristics for the two event days described in this manuscript.

	WSR-88D (KTLX)	TDWR (OKC)	NWRT
Complete volume scan frequency	252 s	~ 210 s*	34 s
Beam width (deg)	0.95°	0.5 °	1.5° – 2.1°
Azimuthal sampling	1.0°	1.0°	1.0°
Gate spacing	250 m	150 m	240 m
Elevation angles	14	9	14

Table 1: Radar sampling characteristics for the platforms sampling the microburst events of 10–11 July 2006. (*) The TDWR conducted one low-altitude scan approximately every 60 s.

As shown by Heinselman et al. (2006), the NWRT PAR can increase the volume scan rate for a specific storm by reducing the

azimuthal sector that contains the storm using its electronically steered antenna. However, in this case a 90° sector was sampled rather than focusing on specific storms which would have reduced the volume scan rate further.

3. Microburst events

The atmosphere in central Oklahoma on 10 and 11 July 2006 was characterized by moderate CAPE (2000 J kg⁻¹ to 2500 J kg⁻¹), weak winds aloft, and an elevated dry layer at about 4.5 km Mean Sea Level. Downdraft convective available potential energy (DCAPE; Gilmore and Wicker 1998), a measure of the atmosphere's instability to downdrafts, was approximately 1100 J kg⁻¹ on 10 July and 1500 J kg⁻¹ on 11 July.

a. 10 July 2006

The 10 July 2006 environment was characterized by several lines and clusters of small convective cells along with a few embedded stronger cells and numerous interacting outflow boundaries. One storm that produced a strong outflow was located to the south/southwest of all three radars, approximately 15 km from the PAR, 17 km from the TDWR, and 34 km from the WSR-88D. The PAR detected a new core aloft at 194112 UTC, and this cell produced a strong outflow sampled near the surface of 30 ms⁻¹ at 195600 UTC. This storm was fully sampled by the PAR a total of 23 times from the first detection of the core aloft to the outflow time. By way of comparison, the WSR-88D completed only 3 volume scans in the same period of time and did not sample the peak outflow. For rapidly-evolving storm cells, the faster scanning speed of the PAR captured storm evolution features that may not be sampled by a WSR-88D.

Figure 1 shows data from 4 of the 23 PAR volume scans. The upper-left of each image shows the vertical reflectivity profile of the storm cell, while the lower-left shows the vertical profile of linear least-squares derivative (LLSD) radial divergence (Smith and Elmore 2004). The upper-right and lower-right images show the reflectivity and radial divergence fields, respectively, at the 0.5° elevation angle. The LLSD radial divergence field is typically very noisy outside of storm regions, but within a storm region it is useful for identifying areas of convergence and divergence.

At 194220 UTC (Figure 1a), a new reflectivity core began to develop aloft at about 6 km vertical (hereafter, Z) and 1 km from the left of the image (hereafter, X). Beneath the core at X = 0.5 km, Z < 0.5 km, an area of radial convergence (negative radial divergence; blue) indicated convergence at the base of the updraft. To the immediate right, centered on X = 2 km, a storm cell in the latter half of its life cycle extended to the surface with a small area of weak divergence apparent at its base. An area of divergence was located near the storm top at X = 1 km, Z = 7 km, but the storm top was not fully sampled by the PAR in this case.

At 194617 UTC (Figure 1b), the core had elongated and descended, with the highest reflectivity values at X = 4 km between Z = 2 km and Z = 6 km. Strong, deep convergence was indicated throughout the depth of the reflectivity core. The convergence at X = 2 km, Z < 0.5 km and the weak echo region at X = 2 km, Z = 4 km suggest an updraft at this location. A first, weak outflow pulse occurred at 195015 UTC (Figure 1c), as the convergence aloft continued to increase. At 195600 UTC (Figure 1d), a very strong gust was indicated in the radial velocity field (Figure 2), as the storm moved closer to the radar and decayed. The shallow outflow was not as apparent in the KTLX data as in the PAR and TDWR data, partially because the beam had propagated farther away from the surface at the longer range (34 km from KTLX versus 15 km from PAR) but also because the maximum velocity measurement occurred temporally between KTLX low-altitude elevation scans.

b. 11 July 2006

Convective activity in Central Oklahoma was not as widespread on 11 July as on the previous day. However, one storm sampled by all three radars produced a 33 ms⁻¹ gust (as measured by a storm spotter) in Lincoln County, OK at 0151 UTC on 12 July. This storm cell was located 55 km from the PAR, 57 km from the TDWR, and 36 km from the WSR-88D. As a result of the farther ranges from the radar, the maximum outflow was not well-sampled by any radar.

Figure 3.a (013729 UTC) shows a brief bounded weak echo region as the storm cell developed near X = 6 km, Z = 5 km, which coincided with strong storm-top divergence

between $Z = 6$ km and $Z = 9$ km. The storm evolution was much the same as in the 10 July case. At 014610 UTC, a deep layer of mid-altitude convergence and descending reflectivity core exist at $X = 11$ km. The low-altitude divergence signature appeared most clearly in the TDWR data and coincided with the maximum reported wind gust at 015150 UTC. Although the low-level outflow was not well-sampled with any radar, the microburst precursor signatures aloft were similar to the 10 July case.

Summary

Examination of the data collected with the NWRT PAR shows the temporal evolution of features that cannot be easily sampled with a beam from a mechanically steered parabolic dish. In both cases, microburst precursors identified in previous studies were easy to visualize and quantify with the PAR data. At shorter ranges from radar on the 10 July case, the evolution of the outflow is well-sampled both spatially and temporally by the NWRT PAR. LLSD divergence derived from the radial velocity field was useful in assessing the convergence / divergence profile of the storm.

We intend to collect many additional cases of microbursts and other hazardous weather events sampled with the NWRT PAR as opportunities arise. This sensor shows great promise in improving the detection and diagnosis of hazardous weather features that evolve rapidly, such as microbursts and tornadoes.

Acknowledgements

We acknowledge the support of our various organizations in funding and helping to implement this national facility. This paper was funded by NOAA/Office of Oceanic and Atmospheric Research under NOAA-University of Oklahoma Cooperative Agreement #NA17RJ1227, U.S. Department of Commerce (DOC). The statements, findings, conclusions, and recommendations are those of the authors and do not necessarily reflect the views of NOAA or the U.S. DOC. For this paper, we

especially thank the leadership of Doug Forsyth and the dedicated work of Mark Benner, Dan Suppes, Kurt Hondl, Mike Jain, Ric Adams, and John Thompson for their assistance with data collection, archiving, and display.

References

- Eilts, M. D., J. T. Johnson, E. D. Mitchell, R. J. Lynn, P. Spencer, S. Cobb, and T. M. Smith, 1996: Damaging Downburst Prediction and Detection Algorithm for the WSR-88D. Preprints, *18th Conf. on Severe Local Storms*, San Francisco, CA, Amer. Meteor. Soc., 541–545.
- Gilmore, M.S. and L.J. Wicker, 1998: The influence of midtropospheric dryness on supercell morphology and evolution. *Mon. Wea. Rev.*, **4**, 943-958.
- Heinselman, P., D. Prieznitz, K. Manross, and R. Adams, 2006: Comparison of storm evolution characteristics: the NWRT and WSR-88D. *Preprints, 23rd Conf. on Severe Local Storms*, St. Louis, MO, AMS, CD-ROM, 14.1.
- Roberts, R. D., and J. W. Wilson, 1989: A proposed microburst nowcasting procedure using single-Doppler radar. *J. Appl. Meteor.*, **28**, 285–303.
- Smith, T.M. and K. L. Elmore, 2004: The use of radial velocity derivatives to diagnose rotation and divergence. *Preprints, 11th Conf. on Aviation, Range, and Aerospace*, Hyannis, MA, Amer. Meteor. Soc., CD-ROM, P5.6.
- , ---, and S. A. Dulin, 2004: A damaging downburst prediction and detection algorithm for the WSR-88D. *Wea. and Forecasting*. **19**: 240-250, Amer. Met. Soc.
- Wolfson, M.M., R.L. Delanoy, B.E. Forman, R.G. Hallowell, M.L. Pawlak, and P.D. Smith, 1994: Automated microburst wind-shear prediction. *The Lincoln Laboratory Journal*, **7**, 399-426.

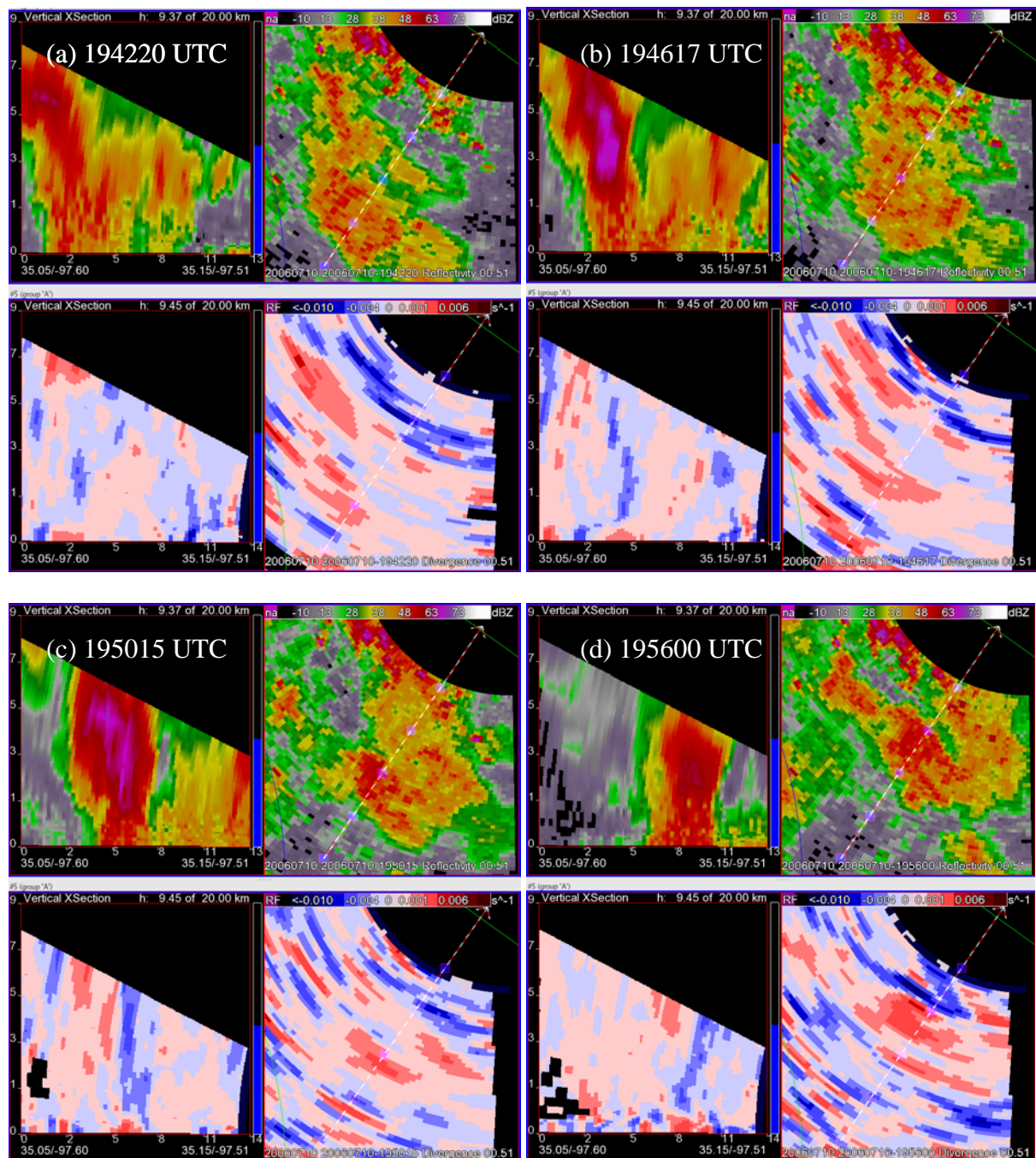


Figure 1: NWRT PAR data showing the evolution of a strong microburst event on 10 July 2006. For each image, the upper-left is the vertical profile of reflectivity (scale in km) along the cross-section indicated by the dashed line in the upper-right image of reflectivity at the 0.5° elevation angle. The lower-left is the vertical cross-section of LLSD radial divergence along the same line, and the lower-right is the divergence at the 0.5° elevation angle.

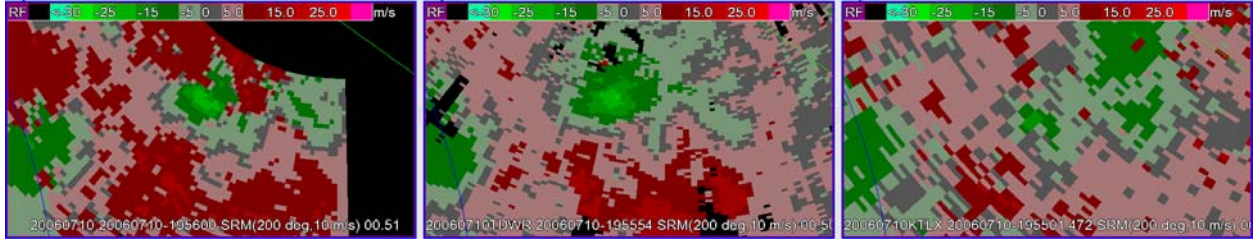


Figure 2: Storm-relative radial velocity for the NWRT PAR (left), OKC TDWR (middle), and KTLX WSR-88D (right). All radars are located to the NNE or NE. Each image is centered on the divergent microburst signature near the same time.

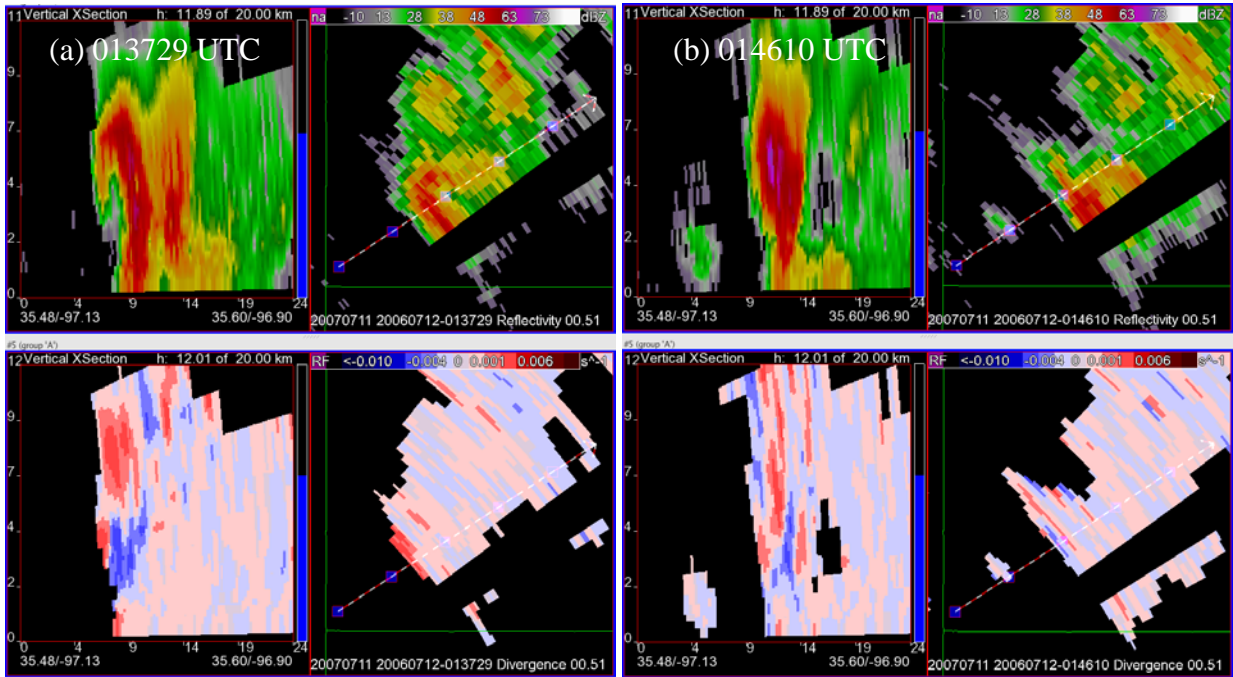


Figure 3: Same as figure 1, except for 12 July 2006. Note that the horizontal and vertical scale is slightly larger than figure 1.

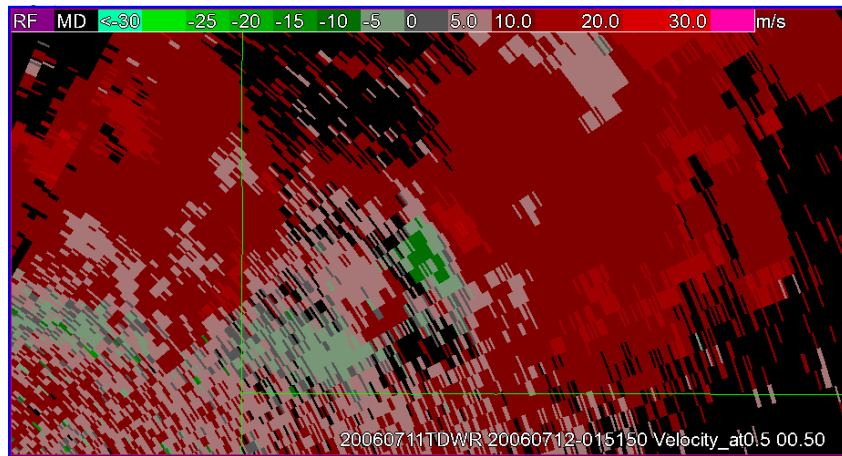


Figure 4: TDWR radial velocity data showing a divergence signature at the time of the 33 ms^{-1} measured wind gust.